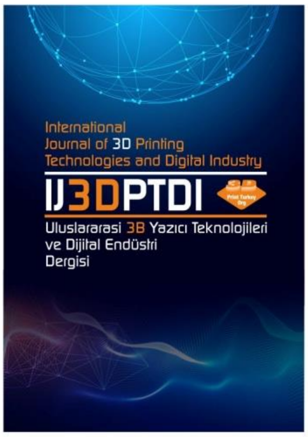

ULUSLARARASI 3B YAZICI TEKNOLOJİLERİ
VE DİJİTAL ENDÜSTRİ DERGİSİ

INTERNATIONAL JOURNAL OF 3D PRINTING TECHNOLOGIES AND DIGITAL INDUSTRY

ISSN:2602-3350 (Online)

URL: https://dergipark.org.tr/ij3dptdi

INVESTIGATION OF THE LOAD-BEARING CAPACITY OF Co-Cr LATTICE STRUCTURES FABRICATED BY SELECTIVE LASER MELTING

Yazarlar (Authors): Nazim Babacan*, Hubannur Seremet

Bu makaleye şu şekilde atıfta bulunabilirsiniz (To cite to this article): *Babacan N., Seremet H., "Investigation of The Load-Bearing Capacity of Co-Cr Lattice Structures Fabricated by Selective Laser Melting" Int. J. of 3D Printing Tech. Dig. Ind., 6(2): 286-291, (2022).*

DOI: 10.46519/ij3dptdi.1139802

Araştırma Makale/ Research Article

Erişim Linki: (To link to this article): https://dergipark.org.tr/en/pub/ij3dptdi/archive

INVESTIGATION OF THE LOAD-BEARING CAPACITY OF Co-Cr LATTICE STRUCTURES FABRICATED BY SELECTIVE LASER MELTING

Nazim Babacan[a]*, Hubannur Seremet[a]

[a]Sivas University of Science and Technology, Faculty of Engineering and Natural Sciences, Department of Mechanical Engineering, TURKEY

* *Corresponding Author:* *nazimbabacan@sivas.edu.tr*

(**Received:** 02.07.2022; **Revised:** 25.07.2022; **Accepted:** 16.08.2022)

ABSTRACT

Additively manufactured Co-Cr lattice structures are promising choices especially in medical applications. This study involves the designing and fabrication of a novel lattice structures with FCCZZ (face-centered cubic with exterior and interior vertical struts) unit cell topology. The manufacturability by selective laser melting (SLM) and the load-bearing capacity of this structure were examined by utilizing scanning electron microscope (SEM) observations and uniaxial compression tests. The samples with FCCZ (face-centered cubic with vertical struts) structures were also produced and analyzed for comparison. The designed lattice structures were successfully manufactured by SLM even though an approximately 1.5-2% increase in the theoretical relative density values was observed. The novel FCCZZ samples exhibited superior performance in terms of the load-bearing capacity compared to FCCZ samples by possessing 17% higher specific strength value.

Keywords: Lattice Structures, Selective Laser Melting, Unit Cell Topology, Co-Cr Alloy, Load-Bearing Capacity.

1. INTRODUCTION

A new era has begun in the manufacturing sector with the start of additive manufacturing technology. Complex shaped parts, which cannot be produced by conventional methods, can be easily produced thanks to this technology [1-3]. Lattice structures, which are formed by the combination of unit cells with unique shapes, are one of the most widely studied additively manufactured parts. The geometry of these structures can be easily controlled so that it can be used to adjust the mechanical properties [4]. These lightweight structures have great specifications such as high specific strength and good energy absorption capacity [5, 6]. Moreover, when they are used as implant structures, they lead to alleviate the stress-shielding problem by decreasing the elasticity modulus of the structures [7].

Laser powder bed fusion or in other terms; selective laser melting (SLM) is seen as the most popular metal additive manufacturing method due to its high dimensional accuracy and ability to process a variety of metals and alloys [8, 9]. Desired geometrical shapes are produced by melting the powders layer-by-layer using the laser energy in SLM. Co-Cr alloys have been one of the most preferred alloys to be produced in SLM. These alloys are known for their great mechanical properties, temperature and corrosion resistance and widely used in orthopedics, aerospace, power generation and dental fields [10,11]. Besides, owing to excellent mechanical strength, and good corrosion resistance, Co-Cr alloys are among popular choices for load-bearing implant applications [12]. Therefore, increasing the load-bearing capacity of the Co-Cr lattice structures enhances their potential to be preferred as implant geometries.

It is known that cell topology is markedly significant on the load-bearing capacity of the porous structures [13]. Face-centered cubic (FCC) [14], body-centered cubic (BCC) [15], diamond [16, 17], auxetic [18], and re-entrant [19] are some of the most prevalent strut-based cell topologies produced by SLM. In addition to these structures, body-centered cubic with vertical struts structures (BCCZ), face-centered cubic with vertical struts structures (FCCZ), which have high stiffness and compressive strength along *z*-direction struts, were utilized by several researchers [20-22]. Leary et al. [21] found that FCCZ exhibit higher specific strength than BCCZ lattice structures. Similarly, FCCZ was seen as the most effective topology in terms of strength to mass ratio compared to BCC, BCCZ, and FCC structures as a result of the quasi-static compression tests performed by Maconachie et al. [20].

Very recently, the current authors showed that adding interior vertical struts to the BCCZ Ti-6Al-4V lattice structure increase the specific strength according to the numerical dynamic compression tests [23]. Thus, this modification, i.e., adding extra vertical struts, can be an important option for other lattice types to increase their load-bearing capacities. In this study, FCCZ and a novel design (FCCZZ; face-centered cubic with exterior and interior vertical struts) Co-Cr alloy samples were manufactured by SLM and their quasi-static compressive responses were examined to see the load-bearing effectiveness of the new design.

2. MATERIAL AND METHODS

2.1. Material and Manufacturing

Commercially available ASTM F75 Co-Cr powders (ERMAK A12; ERMAKSAN) with a measured composition of Co 61.6 wt%, Cr 29.0 wt%, Mo 6.1 wt% and Si 0.3 wt% with trace amounts of C were employed in the present work. The particle size of the powder is in the range of 15–45 μm.

The CAD models of FCCZ and FCCZZ lattice structures were generated by Solidworks software. The unit cell sizes of 4 mm was employed and the strut diameter was chosen as 0.6 mm as well as 5×5×5 cell units in *x*, *y*, and *z* directions. The unit cell geometries of the FCCZ and FCCZZ structures are shown in Figure 1 (a) and (b), respectively. Extra vertical struts in the FCCZZ geometry were highlighted with blue color. The lattice compression specimens were fabricated using ERMAKSAN ENAVISION 130 SLM device under argon atmosphere. The general production parameters were selected to be a laser power of 180 W, a hatch spacing of 100 μm, a scanning speed of 600 mm/s, a spot size of 75 μm and a layer thickness of 30 μm. Images of the FCCZ and FCZZ samples produced by SLM are presented in Figure 1 (c) and (d), respectively. Net sample sizes were measured as approximately 20.8 x 20.75 x 20.5 mm^3 with a caliper for all the specimens.

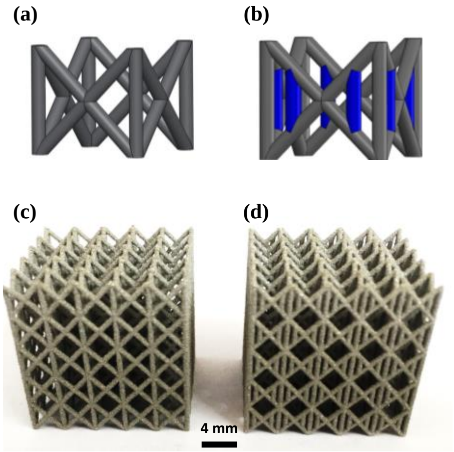

Figure 1. 3D drawings of the unit cells of (a) FCCZ and (b) FCCZZ structures with 4 mm unit cell length and 0.5 mm strut diameter. Images of as-printed (c) FCCZ and (d) FCCZZ compression samples (The scale bar is shown in between the figures).

2.2. Mechanical Tests and Microstructural Characterization

The as-built lattice samples were tested at a strain rate of 10^{-3} s^{-1} using Shimadzu Autograph AGIS-100 kN universal mechanical testing device and each test was repeated three times. Displacement was measured using the crosshead movement.

The morphologies of the as-built samples and the deformation mechanisms of the deformed samples were characterized by a scanning electron microscope (SEM, TESCAN MIRA3 XMU).

3. RESULTS AND DICCUSSION

Figure 2 (a) and (b) show the SEM images of the as-built solid struts by focusing the front view of FCCZ and FCCZZ compression samples, respectively. It seems that the structural integrity was maintained over the surface. Besides, inner struts of FCCZZ were successfully produced without joining with the outer struts (Figure 2(b)). Theoretical relative density values were calculated based on CAD models and tabulated in Table 1. Addition of the interior struts to FCCZ structure caused an increment of %1.7 theoretical relative density. Actual relative densities were measured using the mass, overall dimensions of the as-built samples as well as the theoretical density of 8.35 g/cm^3. SLM-manufactured samples exhibited higher value of density compared to theoretical ones due to adhesion of powder particles as seen in Figure 2 (c) and (d). The addition of extra struts to FCCZ structure increases the error in relative density as similar to the study of Leary et al. [24]. Moreover, the measured strut diameter from the SEM images was found to be approximately 100-150 µm thicker than the designed strut diameter of 0.5 mm and this also clarifies the difference in the theoretical and actual relative densities. The increase in the strut diameter mainly could be attributed unmelted powders which are bonded to strut surfaces (Figure 2 (c) and (d)) and this deviation between the CAD model and the produced structure was also highlighted in many studies [25-28].

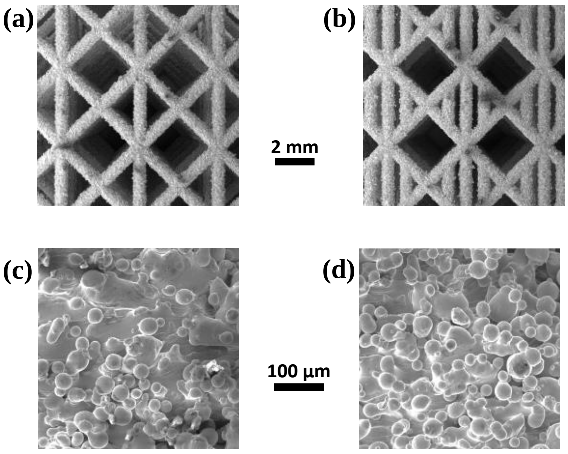

Figure 2. Surface morphology of SLM-manufactured struts belong to (a) FCCZ and (b) FCCZZ structures. A magnified view of the struts focusing on unmelted or partially molten particles of (c) FCCZ and (d) FCCZZ lattices (The scale bars are shown in between the figures).

Table 1. The comparison of the theoretical and actual relative densities of the manufactured samples.

Cell topology	Theoretical relative density (%)	Sample mass (g)	Actual relative density (%)	Error in relative density (%)
FCCZ	8.6	7.34 ± 0.05	9.9	15.1
FCCZZ	10.3	9.13 ± 0.05	12.3	19.4

FCCZ and FCCZZ lattice structures were compressed until 0.5 strain value and the obtained nominal stress-strain curves are displayed in Figure 3. Nominal stress values are calculated with the Equation (1):

$$\sigma = F/A_0 \quad (1)$$

where F is the measured force value and A_0 is the initial cross-sectional area of the lattice sample. It is known that lattice structures exhibit either a bending- or stretch- dominated behavior upon loading according to their topology. Since the initial collapse strength and the modulus of the stretch-dominated structures are higher, they are more suitable for load-bearing applications. Based on the observed decrease in stress after reaching the first peak stress seen in the stress-strain diagrams obtained for both lattice types, it can be said that the structures used in this study exhibit stretch-dominant behavior under loading [29].

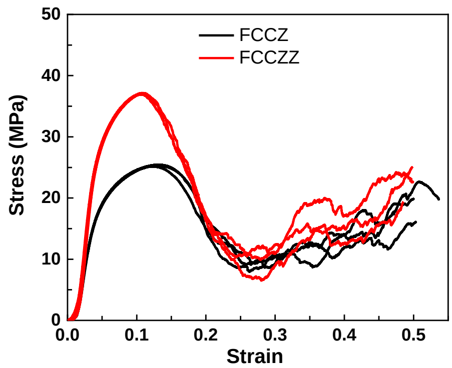

Figure 3. Uniaxial compression stress-strain responses of FCCZ and FCCZZ lattice structures.

Initial elastic part (or elastic-plastic deformation region), fluctuation, and final densification region are the main three stages in the quasi-static stress–strain curves of the lattice specimens [16, 30]. Initial loading causes an elastic deformation and the slope of this linear stage correspond to modulus value. The modulus values of the FCCZ and FCCZZ structures were calculated to be 0.72 ± 0.07 and 1.08 ± 0.07 GPa, respectively. The first peak stress is specified as the ultimate strength. The higher the ultimate strength, the design is stronger for load-bearing applications.

As a second stage, fluctuation starts in the stress-strain curve as a result of the buckling of some individual struts as seen from the SEM images in Figure 4. Different samples that were tested additionally for each lattice type was loaded until 3.5 mm and then unloaded for the further investigation. Local buckling of the struts is clearly seen especially on the struts in the upper as well as right and edge as observed in Figure 4 (a) and (b). Moreover, while some of the interior struts started in some of the struts located in the middle regions as highlighted with red ellipses, FCCZZ structure exhibited higher buckling compared to FCCZ structure in general. Local buckling seen in Figure 4 is also another evidence of the stretch-dominated behavior [31]. While buckling behavior was dominated until the peak stress values, then collapsing was observed layer by layer.

The final densification stage that can be understood from the rapid increase in stress after fluctuation was not seen in these tests, which were done until approximately 10 mm deformation value. Since the relative densities of the investigated lattice structures are not high, it is usual to not to observe densification until 0.5 strain values as seen in the study of Kadkhodapour et al. [32].

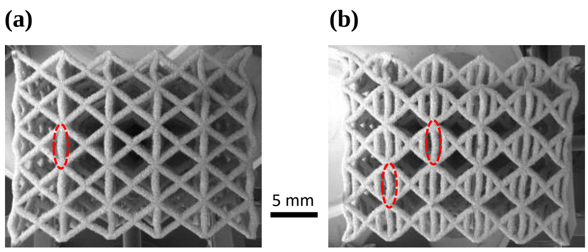

Figure 4. Deformed views of the (a) FCCZ and (b) FCCZZ after 3.5 mm compressive deformation (0.17 strain).

In order to analyze the load-bearing capacity of the novel design, specific strength, which is the ratio of peak stress (ultimate strength) to the apparent density, were calculated and shown in Table 2. It is seen that approximately 17% enhancement was obtained in terms of specific strength with the new FCCZZ design compared to FCCZ lattice structure. This means that FCCZZ samples are more suitable for load-bearing applications.

Table 2. Ultimate and specific strength of the tested Co-Cr samples.

Cell topology	Ultimate strength (MPa)	Apparent density (kg/m^3)	Specific strength (MPa/(kg/m^3))
FCCZ	25.3 ± 0.1	826.65	0.0306 ± 0.0001
FCCZZ	37.1 ± 0.1	1027.05	0.0361 ± 0.0001

4. CONCLUSIONS

In this study, a novel cell topology was designed and analyzed for the usage in load-bearing applications. Adding extra vertical struts to the FCCZ structure greatly increased the ultimate strength under the compression loading. The FCCZZ design showed 17% higher specific strength compared to its counterpart. This work presents a possible way to increase the load-bearing capacity of Co-Cr lattice structures for use in medical implants.

ACKNOWLEDGEMENT

This study was supported by the Alexander von Humboldt (AvH) Foundation Return Fellowship program. The authors would like to thank Aşur Yiğiter for his technical supports.

REFERENCES

1. Geng, X., Ma, L., Liu, C., Zhao, C. and Yue, Z. F., “A FEM study on mechanical behavior of cellular lattice materials based on combined elements”, Materials Science and Engineering A, Volume 712, Pages 188–198, 2018.

2. Balci, A., Aycan, M. F., Usta, Y. and Demir, T. “Seçimli lazer ergitme ile Ti6Al4V ELI alaşımından üretilen trabeküler metal yapıların basma ve basma-kayma dyanımlarının incelenmesi”, Journal of Polytechnic, Volume 24, Issue 3, Pages 903–914, 2021.

3. Saraç, M., Mert, M., Bülbül, İ., Aktitiz, İ., Saygı Yalçın, B. and Varol, R., “Mechanical characterization of 3D printable nanoclay reinforced polymer structures by stereolithography”, Journal of the Institute of Science and Technology, Volume 9, Issue 3, Pages 1584–1593, 2019.

4. Saremian, R., Badrossamay, M., Foroozmehr, E., Kadkhodaei, M. and Forooghi, F., “Experimental and numerical investigation on lattice structures fabricated by selective laser melting process under quasi-static and dynamic loadings”, International Journal of Advanced Manufacturing Technology, Volume 112, Issue 9–10, Pages 2815–2836, 2021.

5. Jin, N., Wang, F., Wang, Y., Zhang, B., Cheng, H. and Zhang, H., "Effect of structural parameters on mechanical properties of Pyramidal Kagome lattice material under impact loading", International Journal of Impact Engineering, Vol. 132, Issue 5, 2019.

6. Gürkan D., Sağbaş B. "Additively manufactured Ti6Al4V lattice Structures for biomedical applications", International Journal of 3D Printing Technologies and Digital Industry, Vol. 5, Issue 2, Pages 155-163, 2021.

7. Xiang, D. D., Wang, P., Tan, X. P., Chandra, S., Wang, C., Nai, M. L. S., Tor, S. B., Liu, W. Q. and Liu, E., "Anisotropic microstructure and mechanical properties of additively manufactured Co–Cr–Mo alloy using selective electron beam melting for orthopedic implants." Materials Science and Engineering A, Vol. 765, Pages 138270, 2019.

8. Boniotti, L., Beretta, S. and Patriarca, L., "Strain concentrations in BCC micro lattices obtained by AM", Procedia Structural Integrity, Vol. 7, Pages 166–173, 2017.

9. Vrána, R., Cervinek, O., Manas, P., Koutný, D. and Paloušek, D., "Dynamic loading of lattice structure made by selective laser melting-numerical model with substitution of geometrical imperfections" Materials, Vol. 11, Issue 11, 2018.

10. Okazaki, Y., Ishino, A. and Higuchi, S., "Chemical, physical, and mechanical properties and microstructures of laser-sintered Co-25Cr-5Mo-5W (SP2) and W-Free Co-28Cr-6Mo alloys for dental applications", Materials, Vol. 12, Issue 24, Pages 4039, 2019.

11. Amanov, A., "A promising post-additive manufacturing surface modification for tailoring gradient nanostructure and harmonic structure in Co–Cr–Mo alloy", Vacuum, Vol. 182, Issue 3, Pages 109702, 2020.

12. Bandyopadhyay, A., Ciliveri, S. and Bose, S., "Metal additive manufacturing for load-bearing implants", Journal of the Indian Institute of Science, Vol. 102, Issue 1, Pages 561–584, 2022.

13. Mazur, M., Leary, M., Sun, S., Vcelka, M., Shidid, D. and Brandt, M., "Deformation and failure behaviour of Ti-6Al-4V lattice structures manufactured by selective laser melting (SLM)", International Journal of Advanced Manufacturing Technology, Vol. 84, Issue 5–8, Pages 1391–1411, 2016.

14. Han, C., Yan, C., Wen, S., Xu, T., Li, S., Liu, J., Wei, Q. and Shi, Y., "Effects of the unit cell topology on the compression properties of porous Co-Cr scaffolds fabricated via selective laser melting", Rapid Prototyping Journal, Vol. 23, Issue 1, Pages 16–27, 2017.

15. Traxel, K. D., Groden, C., Valladares, J. and Bandyopadhyay, A., "Mechanical properties of additively manufactured variable lattice structures of Ti6Al4V", Materials Science and Engineering A, Vol. 809, Pages 140925, 2021.

16. Li, Z. Hua, Nie, Y. Fei, Liu, B., Kuai, Z. Zhou, Zhao, M. and Liu, F., "Mechanical properties of AlSi10Mg lattice structures fabricated by selective laser melting", Materials and Design, Vol. 192, Pages 108709, 2020.

17. Tüzemen, M. Ç., Salamcı, E. and Ünal, R., "Investigation of the relationship between flexural modulus of elasticity and functionally graded porous structures manufactured by AM", Materials Today Communications, Vol. 31, Pages 103592, 2022.

18. Shruti, M., Hemanth, N. S., Badgayan, N. D. and Sahu, S. K., "Compressive behavior of auxetic structural metamaterial for lightweight construction using ANSYS static structural analysis", Materials Today: Proceedings, Vol. 38, Pages 12–17, 2020.

19. Ozdemir, Z., Hernandez-Nava, E., Tyas, A., Warren, J. A., Fay, S. D., Goodall, R., Todd, I. and Askes, H., "Energy absorption in lattice structures in dynamics: Experiments", International Journal of Impact Engineering, Vol. 89, Pages 49–61, 2016.

20. Maconachie, T., Leary, M., Tran, P., Harris, J., Liu, Q., Lu, G., Ruan, D., Faruque, O. and Brandt, M.,"The effect of topology on the quasi-static and dynamic behaviour of SLM AlSi10Mg lattice structures", International Journal of Advanced Manufacturing Technology, Vol. 118, Issue 11–12, Pages 4085–4104, 2022.

21. Leary, M., Mazur, M., Elambasseril, J., McMillan, M., Chirent, T., Sun, Y., Qian, M., Easton, M. and Brandt, M., "Selective laser melting (SLM) of AlSi12Mg lattice structures", Materials and Design, Vol. 98, Pages 344–357, 2016.

22. Hacisalihoğlu, İ., Yildiz, F. and Çelik, A., "Experimental and numerical investigation of mechanical properties of different lattice structures manufactured from medical titanium alloy by using laser beam-powder bed fusion", Journal of Materials Engineering and Performance, Vol. 30, Issue 7, Pages 5466–5476, 2021.

23. Seremet, H., Babacan, N., "Investigating the Dynamic compression response of a novel lattice topology via finite element analyses", 2nd

International Symposium on Light Alloys and Composite Materials, Karabuk, Turkey, Pages 44-47, 2022.

24. Leary, M., Mazur, M., Williams, H., Yang, E., Alghamdi, A., Lozanovski, B., Zhang, X., Shidid, D., Farahbod-Sternahl, L., Witt, G., Kelbassa, I., Choong, P., Qian, M. and Brandt, M., "Inconel 625 lattice structures manufactured by selective laser melting (SLM): Mechanical properties, deformation and failure modes" Materials and Design, Vol. 157, Pages 179–199, 2018.

25. Al-Saedi, D. S. J., Masood, S. H., Faizan-Ur-Rab, M., Alomarah, A. and Ponnusamy, P., "Mechanical properties and energy absorption capability of functionally graded F2BCC lattice fabricated by SLM", Materials and Design, Vol. 144, Pages 32–44, 2018.

26. Qiu, C., Yue, S., Adkins, N. J. E., Ward, M., Hassanin, H., Lee, P. D., Withers, P. J. and Attallah, M. M., "Influence of processing conditions on strut structure and compressive properties of cellular lattice structures fabricated by selective laser melting", Materials Science and Engineering A, Vol. 628, Pages 188–197, 2015.

27. Riva, L., Ginestra, P. S. and Ceretti, E., "Mechanical characterization and properties of laser-based powder bed–fused lattice structures: a review", International Journal of Advanced Manufacturing Technology, Vol. 113, Issue 3–4, Pages 649–671, 2021.

28. Dursun, A. M., Tüzemen, M. Ç., Salamci, E., Yılmaz, O. and Ünal, R., "Investigation of compatibility between design and additively manufactured parts of functionally graded porous structures", Journal of Polytechnic, 2021.

29. Alomar, Z. and Concli, F., "A Review of the Celective laser melting lattice structures and their numerical models", Advanced Engineering Materials, Vol. 22, Issue 12, Pages 1–17, 2020.

30. Jin, N., Wang, Y., Cheng, H., Cheng, X. and Zhang, H., "Strain rate and structure dependent behavior of lattice structures of a titanium alloy fabricated by selective laser melting", Journal of Dynamic Behavior of Materials, Vol. 8, Issue 1, Pages 57-72, 2022.

31. Deshpande, V. S., Ashby, M. F. and Fleck, N. A., "Foam topology: Bending versus stretching dominated architectures", Acta Materialia", Vol. 49, Issue 6, Pages 1035–1040, 2001.

32. Kadkhodapour, J., Montazerian, H., Darabi, A. C., Anaraki, A. P., Ahmadi, S. M., Zadpoor, A. A. and Schmauder, S., "Failure mechanisms of additively manufactured porous biomaterials: Effects of porosity and type of unit cell", Journal of the Mechanical Behavior of Biomedical Materials, Vol. 50, Pages 180–191, 2015.